The Astrophysical Journal, 657:1042–1045, 2007 March 10

THE RADIATIVE PATTERN AND ASYMMETRY OF IRC +10216 AT 11 μm MEASURED WITH INTERFEROMETRY AND CLOSURE PHASE

A. A. Chandler, K. Tatebe, D. D. S. Hale, and C. H. Townes
Space Sciences Laboratory and Department of Physics, University of California, Berkeley, CA;
chandler@ssl.berkeley.edu, tatebe@ssl.berkeley.edu, david@isi.mtwilson.edu, cht@ssl.berkeley.edu
Received 2006 July 21; accepted 2006 November 7

ABSTRACT

The unusual source IRC +10216 is the brightest stellar object at mid-infrared wavelengths in the northern hemisphere. Adding to its distinctiveness, the dust around IRC +10216 almost completely enshrouds the star and has an extremely complex distribution. We report the imaging of IRC +10216 at 11.15 μm with three telescopes and the closure phase at two different stellar phases. Three-baseline interferometry data from a linear array of telescopes is used to create a one-dimensional image of the star and circumstellar dust. The two epochs over which data have been taken provide information at different position angles, which yields some insight into the two-dimensional structure of IRC +10216. Specifically, we observe two areas of peaked intensity. The first is 66 ± 4 mas to the west and 160 ± 51 mas to the south of the star, and the second is 227 ± 8 mas to the east and 94 ± 57 mas to the south. These two features can explain most of the observed asymmetry.

Subject headings: infrared: stars — stars: AGB and post-AGB — stars: individual (IRC +10216) — stars: mass loss — techniques: interferometric

1. INTRODUCTION

IRC +10216 (CW Leo) is a carbon-rich, long-period variable. It has an exceptionally high mass loss rate, on the order of $\sim 10^{-5}\ M_{\odot}\ \mathrm{yr}^{-1}$, and its variations appear to be somewhat irregular. Also, the surrounding intensity distribution is noticeably asymmetric. These peculiarities support the theory that IRC +10216 is in transition from an asymptotic giant branch (AGB) star to a planetary nebula. IRC +10216 is well studied, and maps of intensities at near-infrared wavelengths have been made with lunar occultation (Richichi et al. 2003; Chandrasekhar & Mondal 2001), coronagraphic analysis (Murakawa et al. 2002), and speckle/masking interferometry (Tuthill et al. 2000, 2005; Weigelt et al. 1998, 2002; Osterbart et al. 2000). Visibilities have previously been measured with the two-element Infrared Spacial Interferometer (ISI) by Danchi et al. (1994); however, at that time, the ISI was not able to detect asymmetries.

Measurements reported here were made with the updated ISI, which consists of three moveable telescopes with 65 inch (1.65 m) apertures. The system uses heterodyne detection with $^{13}CO_2$ lasers as local oscillators. The earlier two-telescope ISI has been fully described by Hale et al. (2000). For current observations, the telescopes were located in an east-west linear configuration, with baselines of approximately 4, 8, and 12 m. The bandwidth of the heterodyne detection is quite narrow, approximately 0.17 cm^{-1} or ± 2.6 GHz, which allows the avoidance of spectral lines due to molecules surrounding the source. At 11.15 μm, radiation is detected not only from warm dust, which can also be seen in the near-infrared, but also from dust that is too cool to be well detected at the shorter wavelengths. In addition, the wavelength used is long enough to penetrate the dust and thus directly detect the stellar radiation.

Measurements include visibility values for the three baselines and phase of the three fringes. Taking three visibilities at once permits more internally consistent data than were possible by patching together data from several two-telescope baseline configurations. This also allows the calibrations to be double checked, to a degree, by making sure the data from all three baselines line up to form one continuous curve. The exceptionally small error bars of the IRC +10216 data, as seen in Figures 1 and 2, allow the relative calibration between baselines to be determined with high confidence. Also, with phase-sensitive detection in three telescopes, the closure phase was obtained by summing the phases of fringes for all three baselines (Hale et al. 2003).

2. OBSERVATIONS

Observations of IRC +10216 were made on 2004 November 23 and on 2006 January 11, 13, and 21. Visibility data for both years are shown in Figure 1, and closure phase data are given in Figure 2. There are differences between the two curves because the variable star was at a different luminosity phase for each epoch, and also because the dust may have moved appreciably between measurements. Both these effects are likely explanations for some of the differences observed between the two data sets. The star's period is approximately 638 days (Tuthill et al. 2000), and its luminosity phase is determined from measurements of flux at near-infrared wavelengths (Taranova & Shenavrin 2004). Our best estimate for IRC +10216's luminosity phase is $\Phi = 0.09$ for 2004 November 23 and $\Phi = 0.75$ for 2006 January 11–21. The luminosity phase, Φ, is parameterized from 0 to 1, where 0 is the maximum, and 1 represents the completion of the cycle at maximum again. Subsequent cycles can be represented by increasing integer values. Relative flux intensity in 2006 compared to 2004, as measured by the ISI, was 0.80 ± 0.04. This ratio was obtained by calibrating the power received during each set of observations against the power of the star α Tau. The ISI ratio is used to determine the relative fluxes in Figure 4.

3. METHODS

The methods used for obtaining visibility phase and images from the visibility and closure phase are fully explained in Tatebe et al. (2006). The visibility data are fairly complete in one dimension, with only the star remaining unresolved at the highest spatial frequencies. This means that most of the data are available in the range of spatial frequencies that reveal dust shell information.

Smooth curves can easily be fit to both the visibility and closure phase data within the small error bars associated with these

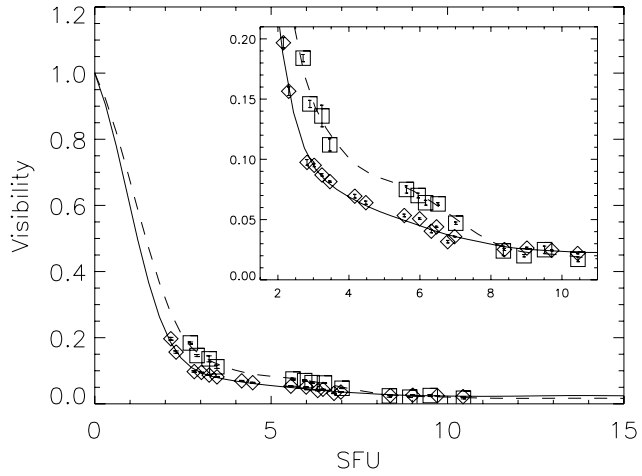

FIG. 1.—Visibility curves of IRC +10216. The diamonds are data taken in 2004, and the solid line is the fit to the curve used for the image. The squares represent data from 2006, and the dashed line is the fit. The unit along the horizontal axis is spatial frequency units (SFU), which equal 10^5 cycles rad^{-1}. The inset plot zooms in on the aforementioned data points.

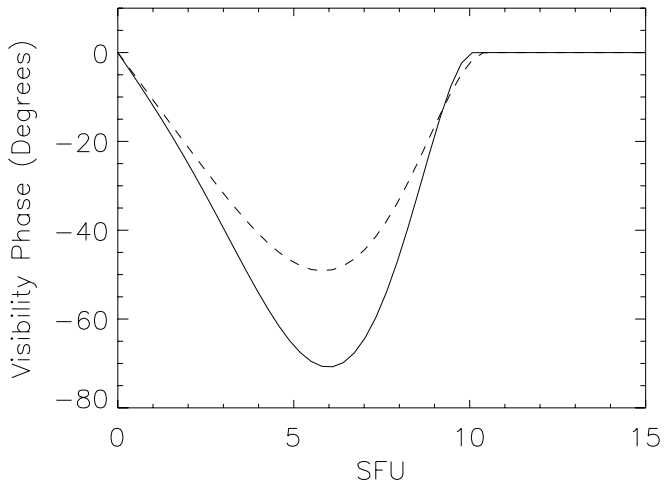

FIG. 3.—Visibility phase for IRC +10216 derived from closure phase measurements. The solid line is the reconstructed phase from 2004 data, and the dashed is from 2006 data.

measurements. The complete visibility phase curve can be determined using the fit to the closure phase data and applying the constraint that the visibility phase returns to zero at high frequencies, which assumes that the star is a uniform disk. Therefore, from a curve fit to the closure phase data, the phase for each individual baseline, undisturbed by atmospheric effects, can be derived. Since the data represent information in one direction (east-west), one-dimensional images of the object are constructed by inverse Fourier transforming the complex visibility curves. The visibility phase is parameterized such that a nonzero phase represents a shift in a Fourier component of the image relative to the center of intensity.

4. RESULTS

Figure 1 plots the visibility for all three baselines versus resolution for both sets of observations. Resolution is measured in spatial frequency units (SFU); where 1 SFU equals 10^5 cycles rad^{-1}. Figure 2 shows the closure phase measurements as a function of SFU for the shortest baseline, labeled SFU (1-2). The error bars are generally smaller than the symbols used to represent the data. Curves have been fit to the data to describe the expected behavior of the visibility outside the measured range of spatial frequencies. For spatial frequencies lower than those measured, the visibility curve has been projected back to unity at 0 SFU. For high spatial frequencies, above ~10.5 SFU, it is assumed that the dust is resolved and the radiation is only from the star, which is symmetric. The fits are shown in Figures 1 and 2 by the solid and dashed lines for 2004 and 2006, respectively. The visibility phase, as a function of spatial frequency, is shown in Figure 3. The images are shown in Figure 4.

The present baselines do not yield high enough resolution to resolve the star. The maximum resolution is about 100 mas, and the flattening of the visibility curve near the highest spatial frequencies measured (~10.5 SFU) indicates a stellar diameter smaller than that. This also makes the existence of a companion star of substantial intensity unlikely. A uniform circular disk of 50 mas diameter is assumed for the star. It is represented in Figure 4 by a sharp central peak. Any reasonable size assumed for the star

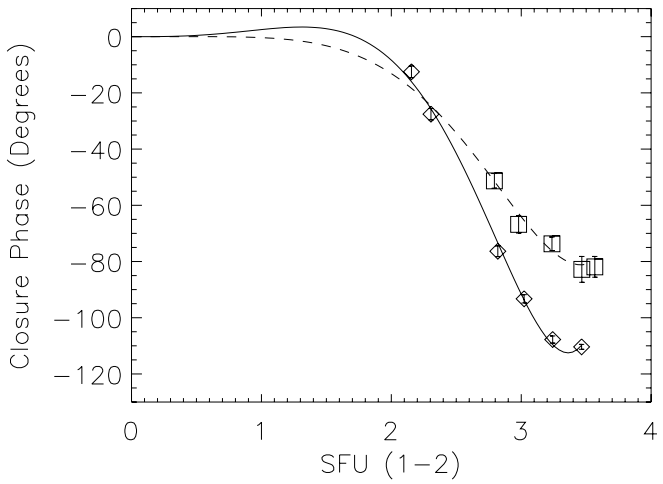

FIG. 2.—Closure phase curves for IRC +10216. The diamond points represent data taken in 2004, and the solid line is the fit to the curve used for the image. The squares represent data from 2006, and the dashed line is the fit. The horizontal axis is in terms of SFU (1-2) (spatial frequency units as measured by the shortest baseline), which equal 10^5 cycles rad^{-1}.

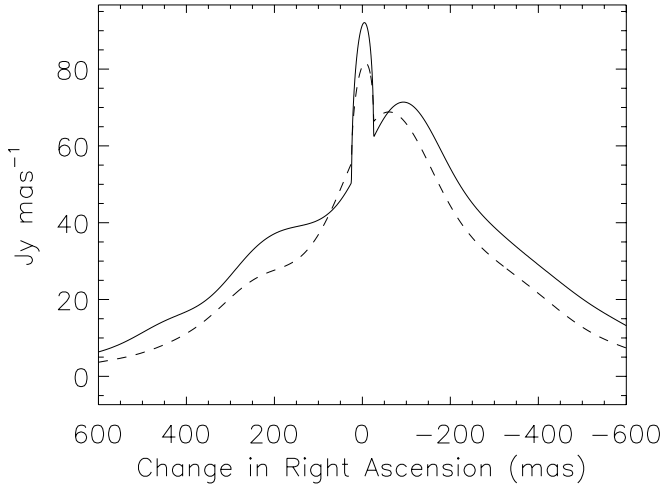

FIG. 4.—One-dimensional profile of the 11 μm intensity of IRC +10216. These images show one-dimensional projections of the two-dimensional intensity distribution. The solid line is the image from 2004 data, and the dashed line is for 2006. We assume the central star to be a uniform disk of 50 mas in diameter, which is represented by the sharp peak. The relative heights give a ratio of 0.8 for the total flux of the 2006 data to the 2004 data. East is to the left in this figure.

would not change the shape of the remainder of the curve of the dust distribution shown in Figure 4. Other stellar sizes would simply vary the width and height of the narrow peak, which represents the star. The total luminosity of the star remains constant at about 2%, while the other 98% of the radiation comes from the dust, as seen by the flattening of the curve in Figure 1.

The images for 2004 and 2006 clearly differ both in relative intensity of the star compared to that of the dust and also in the angular extent of the radiation from the dust. These variations are naturally associated with the stellar phase, which is somewhat further from maximum in 2006 than in 2004. The lower stellar luminosity in 2006 means the dust was cooler, and this cooling should mean that the fractional decrease in dust luminosity becomes greater with increasing distance from the star. Figure 4 shows this to be the case.

There is a noticeable peak $\sim$100 mas to the west of the star in the intensity plot for 2004, and the 2006 data shows this same peak at $\sim$60 mas from the star. There is also another smaller increase in flux at $\sim$200 mas to the east of the star in the plot for 2004. In 2006 this increase appears somewhat weaker and is $\sim$230 mas from the star.

There are at least two possible explanations for the difference in dust distribution between the two epochs. The first is that the dust moved in the time elapsed from 2004 November 23 to 2006 January 11–21. Assuming the dust moves perpendicularly to the line of the sight with a velocity of 20 km s^{-1}, and that the distance to IRC +10216 is 150 pc (cf., Tuthill et al. 2000), it would change its angular position by $\sim$32 mas. Hence, dust motions are a possible cause of the observed changes in angle, which may change $\sim$30–40 mas between observations. However, both dust peaks would have to move in the same direction and with quite high velocity perpendicular to the line of sight. Furthermore, dust is generally expanding around a star rather than moving closer to it, as the most intense peak appears to do between 2004 and 2006. Therefore, this explanation seems unlikely to completely account for the situation.

A more reasonable cause of the position difference of these intensity bumps is the 15° difference in the average position angles for the observations during the two periods. Although the range of position angles overlap slightly, the general change in location of the bright spots can be assumed to represent the general change in profile of the star with position angle. Distortions caused by changes in position angle are discussed in § 5. The shifts observed are consistent with the eastern bump corresponding to a dust cloud to the southeast, and the western bump to another dust cloud somewhat closer to the star and to the southwest. Specifically, a dust cloud 227 ± 8 mas to the east and 94 ± 57 mas to the south of the star would appear 200 mas toward the east when seen at a position angle of 103°, as in 2004, and 230 mas toward the east when seen at a position angle of 88°, as in 2006. A cloud 66 ± 4 mas to the west and 160 ± 51 mas to the south would produce the apparent changes in the western intensity bump from 2004 to 2006. The errors represent the range of positions that can be triangulated based on the variations in position angle within each set of data. Accounting for the change in position angle can contribute some two-dimensional information rather than a simple one-dimensional picture. It provides likely positions for two different dust clouds, which emit substantial 11.15 μm radiation.

It is currently assumed that the flux is due only to a single AGB star and its circumstellar dust. The total flux of 47,500 Jy used for the 2004 data (Ochsenbein et al. 2000) was obtained from an *IRAS* 12 μm measurement and was not necessarily taken at the same phase, but is an acceptable estimate of the flux used to give a scale to the intensity axis of Figure 4. Relative heights of the two intensity distributions (2006 to 2004) produce the ratio of 0.8 as measured by ISI for the integrated intensities at the two different stellar phases. The plot in Figure 4 is limited to a total width of 1.2″, slightly less than the full width at half-maximum of the beam, which is 1.4″. The model shown assumes a constant beam over the image observed.

5. DISCUSSION

While many differences are possible between near-infrared data and our measurements in the mid-infrared, there is an encouraging similarity between data from the two wavelengths. A handful of observations in the *H*, *J*, and *K* bands find a strong peak to the southwest and a weaker peak to the southeast, just as we observe in the *N* band. The southwestern peak described in § 4 agrees (to within error) with peak A from Weigelt et al. (1998), if point B, as is accepted in a later paper (Weigelt et al. 2002), is taken to be the star. This gives some affirmation that the interpretation of Weigelt et al. (2002) of point B as the star is correct, since the present 11 μm results very clearly locate the star. Our findings roughly correlate with the data taken at a phase of $\Phi = 3.93$ in the *J* band by Weigelt et al. (2002), although the results do not align as nicely as with the *H*- or *K*-band measurements of that paper, where the distance between the dust peaks shrinks somewhat. The data taken at a phase of $\Phi = 1.61$ by Weigelt et al. (2002) do not agree, with the southeast peak disappearing and being replaced by another to the northeast, in contrast to findings by Tuthill et al. (2005). Lack of correlation may in part be because of the rapid changes with time reported in these papers, as well as the substantial difference in wavelength. Also, the two epochs in Weigelt et al. (2002) are separated by more than 4 yr, in contrast to 1 yr for the ISI data. The same general structures, but not precise alignments, are found in Men'shchikov et al. (2002) and Osterbart et al. (2000). A further complication exists because the circumstellar dust is so thick that the position of the star in the near-infrared is not explicitly known, nor agreed upon from publication to publication. While the distribution of intensity from the dust is very roughly symmetric, its clustering around the star is not. The flattening of the 11.15 μm visibility curve indicates that at this wavelength, in contrast to the near IR, the dust does not significantly mask the star's position, allowing its location relative to the dust to be determined with high confidence.

To create these one-dimensional images, the change in position angle of the star over a night of observation is assumed to have little impact on the measured curves. While this is approximately true, there are some complications. The average position angle for the 2004 observations was 103°, but the angle varied ±11°. The average position angle for the 2006 observations was 88°, but variations were ±7°. The difference of 15° in average position between the two epochs is due to the fact that in 2004 the star was observed mostly toward the east, whereas in 2006 it was mostly toward the west.

The two data sets presented here were taken only when the star was rising for 2004 and only when it was setting in 2006. These images represent, roughly, what the average profile should look like over the span of position angles at which the measurements were taken. Thus, even though there may be some distortion of the shape from the true profile at the average position angle, the general apparent motion of the peaks will be in the correct direction.

Certainly, some distortions will result from the low spatial frequency data being taken at higher position angle separations for the two different years than the high-frequency data. This is because the lowest spatial frequencies are recorded when the star is farthest to the east in 2004 and to the west in 2006. Because of this, small structures in the profile may move less than similarly

located large structures. This may bias the parallax measurements so that, in actuality, the large structures are displaced relatively less in the north-south direction for a given observed shift in position, while small structures are displaced relatively farther. While this may distort the locations of structures slightly, the general direction of the shifts observed, as an average, should be consistent with the true configuration of the object. The positions stated should still give a realistic idea of the location of the structures in the dust to within the errors provided.

6. CONCLUSIONS

The asymmetry of the distribution of IRC +10216 's circumstellar material is remarkable and not easily understood. No source of this material or the flux illuminating it is evident other than the single AGB star. This indicates remarkable asymmetry in the emission and/or illumination of the circumstellar material by the star. IRC +10216 is an old and very active star, and it is likely that its instabilities have pushed off or illuminate material in a very asymmetric manner. Both the star and the material surrounding it change rapidly enough that continued measurements over a few years may be able to clarify the dynamics. Currently available interferometry at near- and mid-infrared wavelengths should provide such information.

We hope to soon learn the star's actual diameter and whether it is circular and symmetric. In support of this effort the three telescopes have recently been moved to a triangular configuration, with much longer baselines of $\sim$30 m, in hopes of measuring the stellar size and resolving any photospheric asymmetries.

This research has been supported by the Office of Naval Research, the National Research Foundation, NASA, and the Gordon and Betty Moore Foundation. The authors would like to thank Roger Griffith for his valuable contributions to the maintenance and operation of the ISI.

REFERENCES

Chandrasekhar, T., & Mondal, S. 2001, MNRAS, 322, 356
Danchi, W. C, Bester, M., Degiacomi, C. G., Greenhill, L. J., & Townes, C. H. 1994, AJ, 107, 1469
Hale, D. D. S., Fitelson, W., Monnier, J. D., Weiner, J., & Townes, C. H. 2003, Proc. SPIE, 4838, 387
Hale, D. D. S., et al. 2000, ApJ, 537, 998
Murakawa, K., et al. 2002, A&A, 395, L9
Men'shchikov, A. B., Hofmann, K.-H., & Weigelt, G. 2002, A&A, 392, 921
Ochsenbein, F., Bauer, P., & Marcout, J. 2000, A&AS, 143, 23
Osterbart, R., Balega, Y. Y., Blöcker, T., Men'shchikov, A. B., & Weigelt, G. 2000, A&A, 357, 169
Richichi, A., Chandrasekhar, T., & Leinert, C. 2003, NewA, 8, 507
Taranova, O. G., & Shenavrin, V. I. 2004, Astron. Lett., 30, 549
Tatebe, K., Chandler, A. A., Hale, D. D. S., & Townes, C. H. 2006, ApJ, 652, 666
Tuthill, P. G., Monnier, J. D., & Danchi, W. C. 2005, ApJ, 624, 352
Tuthill, P. G., Monnier, J. D., Danchi, W. C., & Lopez, B. 2000, ApJ, 543, 284
Weigelt, G., Balega, Y. Y., Blöcker, T., Fleischer, A. J., Osterbart, R., & Winters, J. M. 1998, A&A, 333, L51
Weigelt, G., Balega, Y. Y., Blöcker, T., Hofman, K.-H., Men'shchikov, A. B., & Winters, J. M. 2002, A&A, 392, 131